Eur. Phys. J. C (2018) 78:453
https://doi.org/10.1140/epjc/s10052-018-5937-3

THE EUROPEAN PHYSICAL JOURNAL C

Regular Article - Theoretical Physics

An empirical model to determine the hadronic resonance contributions to $\overline{B}^0 \to \overline{K}^{*0}\mu^+\mu^-$ transitions

T. Blake[1], **U. Egede**[2], **P. Owen**[3], **K. A. Petridis**[4], **G. Pomery**[4,a]

[1] University of Warwick, Coventry, UK
[2] Imperial College London, London, UK
[3] Universität Zürich, Zürich, Switzerland
[4] Univeristy of Bristol, Bristol, UK

Received: 23 April 2018 / Accepted: 28 May 2018 / Published online: 6 June 2018

Abstract A method for analysing the hadronic resonance contributions in $\overline{B}^0 \to \overline{K}^{*0}\mu^+\mu^-$ decays is presented. This method uses an empirical model that relies on measurements of the branching fractions and polarisation amplitudes of final states involving $J^{PC} = 1^{--}$ resonances, relative to the short-distance component, across the full dimuon mass spectrum of $\overline{B}^0 \to \overline{K}^{*0}\mu^+\mu^-$ transitions. The model is in good agreement with existing calculations of hadronic non-local effects. The effect of this contribution to the angular observables is presented and it is demonstrated how the narrow resonances in the q^2 spectrum provide a dramatic enhancement to CP-violating effects in the short-distance amplitude. Finally, a study of the hadronic resonance effects on lepton universality ratios, $R_{K^{(*)}}$, in the presence of new physics is presented.

1 Introduction

Decays with a $b \to s\,\ell^+\ell^-$ transition receive contributions predominantly from loop-level, flavour changing neutral current transitions. These transitions are mediated by heavy (short-distance) particles and are suppressed in the Standard Model (SM). Over the last few years, discrepancies have emerged when comparing measurements of the properties of $b \to s\,\ell^+\ell^-$ decays to SM predictions [1–10]. Global analyses of these decays imply that there might be a new vector current which is destructively interfering with the SM contribution to the $b \to s\,\ell^+\ell^-$ decay, producing inconsistency with the SM at the 4–5σ [11–17].

In this paper, the possibility that hadronic resonances are interfering with the short-distance amplitude and mimicking physics beyond the SM is considered. This is because in addition to the short-distance contribution to $b \to s\,\ell^+\ell^-$ decays, the same final state can be obtained through non-local $b \to sq\overline{q}$ transitions, where $q\overline{q}$ denotes a quark-anti-quark pair. An example of such a decay is the decay $\overline{B}^0 \to J/\psi\,\overline{K}^{*0}$, where the J/ψ meson decays into two leptons.[1] As the decay rate of this process is two orders of magnitude larger than its short-distance counterpart, sizeable interference effects are possible far from the J/ψ mass.

The approach presented in this paper models the hadronic contributions originating from charm and light quark resonances as Breit–Wigner amplitudes. This approach is inspired by Refs. [18,19] and is used to describe the hadronic resonances across the full dimuon mass spectrum of $B^0 \to K^{*0}\mu^+\mu^-$ decays. The LHCb collaboration performed a measurement of the interference between the non-local and short-distance components of $B^- \to K^-\mu^+\mu^-$ decays by modelling the hadronic resonance contributions as Breit–Wigner amplitudes [20]. The level of interference was found to be small and the measurement of the short-distance component was found to be compatible with that of previous interpretations.

These non-local contributions are difficult to calculate and to date there is no consensus as to whether the deviations seen in global analyses can be explained by the these intermediate hadronic contributions, or by physics beyond the SM. Differentiating between these two hypotheses is of prime importance for confirming the existence and subsequently characterising phenomena not predicted by the SM. More detailed discussions on this point can be found in Refs. [18,19,21–28].

Due to the more complex amplitude structure of the decay, for each resonant final state there are three relative phases

[a] e-mail: gp14936@bristol.ac.uk

[1] Inclusion of charge conjugate processes is implied throughout this paper unless otherwise noted.

and magnitudes that need to be determined instead of one in the case of the $B^- \to K^-\mu^+\mu^-$ decay. Existing measurements of the branching fractions of $\overline{B}^0 \to J/\psi\,\overline{K}^{*0}$ and $\overline{B}^0 \to \psi(2S)\overline{K}^{*0}$ decays, together with measurements of their polarisation amplitudes [29–32] can be used to assess the impact of these decays to the observables of the $\overline{B}^0 \to \overline{K}^{*0}\mu^+\mu^-$ process, up to a single overall phase per resonance that needs to be determined through a simultaneous fit to both the short-distance and non-local components in the $\overline{K}^{*0}\mu^+\mu^-$ final state. In the absence of such a measurement, scanning over all possible values for the global phase for each resonant final state, results in a prediction of the range of hadronic effects that can be compared to more formal calculations. The angular distribution of the decay $\overline{B}^0 \to \overline{K}^{*0}\mu^+\mu^-$ is sensitive to the strong-phases of non-local contributions, particularly through the observables S_7 and S_9. This sensitivity allows for a data-driven extraction of the non-local parameters of the proposed model.

The level of CP violation in decays such as $\overline{B}^0 \to \overline{K}^{*0}\mu^+\mu^-$ depends on weak- and strong-phase differences with interfering processes, such as $\overline{B}^0 \to J/\psi\,\overline{K}^{*0}$. Therefore, a model for the strong phases of the non-local contributions to $B^0 \to K^{*0}\mu^+\mu^-$ transitions, offers new insight on both the kinematic regions where CP violation might be enhanced, as well as what the level of enhancement could be.

An increasingly large part of the discrepancy in $b \to s\,\ell^+\ell^-$ transitions is being driven by tests of lepton universality in $\overline{B} \to \overline{K}^{(*)}\ell^+\ell^-$ decays [3,33,34]. These deviations cannot be explained by hadronic effects (the J/ψ meson, for example, decays equally often to electrons and muons). Although a significant deviation from lepton-universality would be a clear indication of physics beyond the SM, the precise characterisation of the new physics model still depends on the treatment of hadronic contributions. The angular distribution of $\overline{B}^0 \to \overline{K}^{*0}\ell^+\ell^-$ decays is critical in order to both determine the size of the new physics contribution, as well as to distinguish between models with left- or right-handed currents giving rise to new vector and axial-vector couplings.

This paper is organised as follows: Section 2 describes the model of the non-local contributions as well as the experimental inputs; Section 3 presents the comparison of the model to existing calculations; Section 4 shows how current model uncertainties impact both CP-averaged and CP-violating observables of $\overline{B}^0 \to \overline{K}^{*0}\mu^+\mu^-$ decays, as well as the expected precision of the $\overline{B}^0 \to \overline{K}^{*0}\mu^+\mu^-$ observables using the data that is expected from the LHCb experiment by the end of Run 2 of the LHC; finally in Section 5 there is a discussion of the impact of the non-local contributions in $\overline{B}^0 \to \overline{K}^{*0}\ell^+\ell^-$ and $B^- \to K^-\ell^+\ell^-$ transitions in the presence of lepton-universality violating physics.

2 The model

The differential decay rate of $\overline{B}^0 \to \overline{K}^{*0}\mu^+\mu^-$ transitions, where the $\overline{K}^{*0}$ is a P-wave state and ignoring scalar or timelike contributions to the dimuon system, depends on eight independent observables [35]. Each of these observables is made up of bilinear combinations of six complex amplitudes representing the three polarisation states of the $\overline{K}^{*0}$ for both the left- and right-handed chirality of the dilepton system. The expression for the differential decay rate in terms of the angular observables and their subsequent definition in terms of amplitudes, can be found in Ref. [36]. The decay amplitudes are written in terms of the complex valued Wilson Coefficients C_7, C_9 and C_{10}, encoding short distance effects, and the q^2 dependent form-factors , $F_i(q^2) = (V, A_1, A_{12}, T_1, T_2, T_{23})$ given in Ref. [15], that express the $B \to K^*$ matrix elements of the operators involved in these decays. The coefficient C_9 corresponds to the coupling strength of the vector current operator, C_{10} to the axial-vector current operator and C_7 to the electromagnetic dipole operator. A detailed review of these decays, including the operator definitions and the numerical values of the Wilson Coefficients in the SM, can be found in Ref. [36]. The decay amplitudes in the transversity basis and assuming a narrow K^{*0} can be written as

$$\mathcal{A}_0^{\mathrm{L,R}}(q^2) = -8N\frac{m_B m_{K^*}}{\sqrt{q^2}}\Big\{(C_9 \mp C_{10})A_{12}(q^2) + \frac{m_b}{m_B + m_{K^*}}C_7 T_{23}(q^2) + \mathcal{G}_0(q^2)\Big\}, \tag{1}$$

$$\mathcal{A}_\parallel^{\mathrm{L,R}}(q^2) = -N\sqrt{2}(m_B^2 - m_{K^*}^2)\Big\{(C_9 \mp C_{10})\frac{A_1(q^2)}{m_B - m_{K^*}} + \frac{2m_b}{q^2}C_7 T_2(q^2) + \mathcal{G}_\parallel(q^2)\Big\}, \tag{2}$$

$$\mathcal{A}_\perp^{\mathrm{L,R}}(q^2) = N\sqrt{2\lambda}\Big\{(C_9 \mp C_{10})\frac{V(q^2)}{m_B + m_{K^*}} + \frac{2m_b}{q^2}C_7 T_1(q^2) + \mathcal{G}_\perp(q^2)\Big\}, \tag{3}$$

where m_B, m_{K^*} and m_ℓ are the masses of the B-meson, K^*-meson, and lepton respectively, q^2 denotes the mass of the dimuon system squared, $\lambda = m_B^4 + m_{K^*}^4 + q^4 - 2(m_B^2 m_{K^*}^2 + m_{K^*}^2 q^2 + m_B^2 q^2)$, $\beta_\ell = \sqrt{1 - 4m_\ell^2/q^2}$ and

$$N = V_{tb}V_{ts}^*\sqrt{\frac{G_F^2\alpha^2}{3\times 2^{10}\pi^5 m_B^3}q^2\lambda^{1/2}\beta_\mu}\,. \tag{4}$$

In the above expressions, and for the remainder of this analysis, contributions from right handed Wilson Coefficients have been omitted. These are numerically small or zero in the SM and are not currently favoured by global analyses of

$b \to s\,\ell^+\ell^-$ processes. Following Ref. [15], the form factors are written

$$F^i(q^2) = \frac{1}{1 - q^2/m_{R_i}^2} \sum_{k=0}^{2} \alpha_k^i [z(q^2) - z(0)]^k, \tag{5}$$

where the z function is given by

$$z(t) = \frac{\sqrt{t_+ - t} - \sqrt{t_+ - t_0}}{\sqrt{t_+ - t} + \sqrt{t_+ - t_0}}, \tag{6}$$

with $t_\pm = (m_B \pm m_{K^*})^2$ and $t_0 = t_+(1 - \sqrt{1 - t_-/t_+})$. The parameters m_{R_i} are taken from Ref. [15] and the coefficients α_k^i including their correlations are taken from a combined fit to light-cone sum rule calculations and Lattice QCD results given in Refs. [15,37].

The functions $\mathcal{G}_\lambda(q^2)$ describe the non-local hadronic contributions to the $B^0 \to K^{*0}\mu^+\mu^-$ amplitudes and are given by a simplistic empirical parametrisation inspired by the procedure of Refs. [18–20]. In particular

$$\mathcal{G}_0 = \frac{m_b}{m_B + m_{K^*}} T_{23}(q^2)\zeta^0 e^{i\omega^0} + A_{12}(q^2) \sum_j \eta_j^0 e^{i\theta_j^0} A_j^{\rm res}(q^2), \tag{7}$$

$$\mathcal{G}_\parallel = \frac{2m_b}{q^2} T_2(q^2)\zeta^\parallel e^{i\omega^\parallel} + \frac{A_1(q^2)}{m_B - m_{K^*}} \sum_j \eta_j^\parallel e^{i\theta_j^\parallel} A_j^{\rm res}(q^2), \tag{8}$$

$$\mathcal{G}_\perp = \frac{2m_b}{q^2} T_1(q^2)\zeta^\perp e^{i\omega^\perp} + \frac{V(q^2)}{m_B + m_{K^*}} \sum_j \eta_j^\perp e^{i\theta_j^\perp} A_j^{\rm res}(q^2), \tag{9}$$

where the sum in the above expressions represents the coherent sum of vector meson resonant amplitudes with η_j^λ and θ_j^λ the magnitude and phase of each resonant amplitude relative to C_9. The exact normalisation of the η_j^λ parameters is shown in Appendix A and is chosen such the integral of the sum of the squared magnitudes of the amplitude of a given amplitude produce the correct experimental branching fraction. Similarly, the parameters ζ^λ and ω^λ need to be determined from experimental measurements. In this analysis, the central values of these parameters are set to zero, unless otherwise specified.

The q^2 dependence of each resonant amplitude is given by $A_j^{\rm res}(q^2)$. As indicated from the analysis of the dimuon mass spectrum in $B^- \to K^-\mu^+\mu^-$ decays from Ref. [20], the resonances considered in this analysis are the ρ^0, ϕ, J/ψ, $\psi(2S)$, $\psi(3770)$, $\psi(4040)$ and $\psi(4160)$. Contributions from light-quark resonances are expected to be either CKM- or loop-suppressed compared to final states occurring through charmonium resonances. As experiments accumulate more data, additional broad light-quark states will start becoming statistically significant and can be easily incorporated in the model. For simplicity, $A_j^{\rm res}$ is modelled by a relativistic Breit–Wigner function given by

$$A_j^{\rm res}(q^2) = \frac{m_{{\rm res}\,j}\Gamma_{{\rm res}\,j}}{(m_{{\rm res}\,j}^2 - q^2) - i m_{{\rm res}\,j}\Gamma_j(q^2)}, \tag{10}$$

where $m_{{\rm res}\,j}$ and $\Gamma_{{\rm res}\,j}$ are the pole mass and natural width of the $j^{\rm th}$ resonance and their values are taken from Ref. [38]. The running width $\Gamma_j(q^2)$ is given by

$$\Gamma_j(q^2) = \frac{p}{p_{{\rm res}\,j}} \frac{m_{{\rm res}\,j}}{q} \Gamma_{{\rm res}\,j}, \tag{11}$$

where p is the momentum of the muons in the rest frame of the dimuon system evaluated at q, and $p_{{\rm res}\,j}$ is the momentum evaluated at the mass of the resonance.

This isobar approach, although not rigorous, it provides a model for the strong phase variation of the amplitude across the full q^2 spectrum. This variation can result in sizeable effects even far from the pole of the resonances as discussed in Sect. 4.

It is customary that for each helicity amplitude, the expressions of the non-local components $\mathcal{G}_\lambda$ are recast as shifts to the Wilson coefficient C_9, referred to as $\Delta C_{9\,\lambda}^{\rm total}$. This convention is particularly useful for comparisons with formal predictions of the non-local contributions.

Measurements of $\overline{B}^0 \to V\overline{K}^{*0}$ decays, where V denotes any $J^{PC} = 1^{--}$ state, are only sensitive to relative phases of the three transversity amplitudes. Therefore, the convention used in previous measurements of these modes is such that phases $\theta_\parallel$ and $\theta_\perp$ are defined relative to θ_0. Using this convention, the remaining phase difference of each resonant polarisation amplitude relative to the corresponding short-distance one, is given by θ_0.

2.1 Experimental input

In order to assess the impact of the resonances appearing in the dimuon spectrum of $\overline{B}^0 \to \overline{K}^{*0}\mu^+\mu^-$ decays, knowledge of the resonance parameters η_j and θ_j appearing in Eqs. 7–9 is required. The amplitude analyses of $\overline{B}^0 \to J/\psi\,\overline{K}^{*0}$ and $\overline{B}^0 \to \psi(2S)\overline{K}^{*0}$ transitions performed by the LHCb, BaBar and Belle collaborations [30,31,39] constrain the relative phases and magnitudes of the transversity amplitudes of the resonant decay modes. Combined with the measured branching fractions of these decays by the Belle experiment [30,32], the parameters $\eta_j^{\parallel,\perp,0}$ and $\theta_j^{\parallel,\perp}$ are determined up to an overall phase, θ_j^0, relative to the short-distance amplitude for the $\overline{B}^0 \to \overline{K}^{*0}\mu^+\mu^-$ decay. Similarly, the amplitude components of $\overline{B}^0 \to \phi\overline{K}^{*0}$ transitions have been determined up to an overall phase, through the amplitude

Table 1 Summary of the input values used to model the non-local amplitude components $\mathcal{G}_\lambda$. The input values rely on measurements given in Refs. [20,29–32,40–44]. The phases are measured relative to θ_j^0. As the measurements are given for the decay of the B^0 meson, in order to convert to the decay of the $\overline{B}^0$, the phase $\theta_j^\perp$ given in the table above must be shifted by π

Mode	$(\eta_j^\parallel, \theta_j^\parallel\,[rad])$	$(\eta_j^\perp, \theta_j^\perp\,[rad])$	η_j^0
$B^0 \to \rho^0 K^{*0}$	(1.5, 2.6)	(1.9, 2.6)	5.1×10^{-1}
$B^0 \to \phi K^{*0}$	$(2.5 \times 10^{+1}, 2.6)$	$(3.2 \times 10^{+1}, 2.6)$	$1.0 \times 10^{+1}$
$B^0 \to J/\psi\, K^{*0}$	$(4.9 \times 10^{+3}, -2.9)$	$(6.5 \times 10^{+3}, 2.9)$	$7.1 \times 10^{+3}$
$B^0 \to \psi(2S) K^{*0}$	$(5.3 \times 10^{+2}, -2.8)$	$(8.1 \times 10^{+2}, 2.8)$	$9.6 \times 10^{+2}$
$B^0 \to \psi(3770) K^{*0}$	$(9.3 \times 10^{-1}, -2.9)$	(1.5, 2.9)	1.7
$B^0 \to \psi(4040) K^{*0}$	$(2.9 \times 10^{-1}, -2.9)$	$(5.6 \times 10^{-1}, 2.9)$	6.0×10^{-1}
$B^0 \to \psi(4160) K^{*0}$	$(8.3 \times 10^{-1}, -2.9)$	(2.0, 2.9)	1.8

analyses and branching fraction measurements given in Refs. [40–42].

For the decay $\overline{B}^0 \to \rho^0 \overline{K}^{*0}$, the magnitude of the total decay amplitude is set using the world average branching fraction of this transition [38,43,44]. As no amplitude analysis of this mode has been performed, the relative phases and magnitudes of the transversity amplitudes are taken to be the same as those of the $\overline{B}^0 \to \phi \overline{K}^{*0}$ decay. As the overall contribution of the ρ^0 is expected to be small, this assumption will not impact the main conclusions of this study.

No measurements exist for final states involving the $\psi(3770)$, $\psi(4040)$ and $\psi(4160)$ resonances, denoted as $\overline{B}^0 \to V_\psi \overline{K}^{*0}$. To estimate the contributions of these final states, the relative phases and magnitudes of the transversity amplitudes are taken from the amplitude analysis of $\overline{B}^0 \to J/\psi\, \overline{K}^{*0}$ decays. An approximate value of the branching fraction of each of the $\overline{B}^0 \to V_\psi \overline{K}^{*0}$ modes is obtained by scaling the measured branching fraction of the decay $\overline{B}^0 \to \psi(2S)\overline{K}^{*0}$, with $\psi(2S) \to \mu^+\mu^-$, by the known ratio of branching fractions between $B^+ \to \psi(2S)K^+$ and $B^+ \to V_\psi K^+$ decays, with $V_\psi \to \mu^+\mu^-$, given in Ref. [20]. The values used for the relative amplitudes and phases for each resonant contribution are summarised in Table 1.

3 Model comparisons

The study presented in Ref. [28] provides a prediction of the non-local charm loop contribution to $\overline{B}^0 \to \overline{K}^{*0}\mu^+\mu^-$ decays. It relies on QCD light-cone sum rule calculations of $B \to K^*$ matrix elements for $q^2 \ll 4m_c^4$ and extrapolated to larger q^2 through a hadronic dispersion relation. The extrapolation uses input from experimental measurements of the rate and amplitude structure of $\overline{B}^0 \to J/\psi\, \overline{K}^{*0}$ and $\overline{B}^0 \to \psi(2S)\overline{K}^{*0}$ decays. As this calculation does not account for the factorisable next-to-leading order corrections to the charm loop, all phases of the non-local relative to the short-distance amplitudes are set to zero.

Figure 1 shows the parametrisation of the non-local contributions in the invariant amplitude basis of $\overline{B}^0 \to \overline{K}^{*0}\mu^+\mu^-$ decays given in Ref. [28]. The relation of this amplitude basis

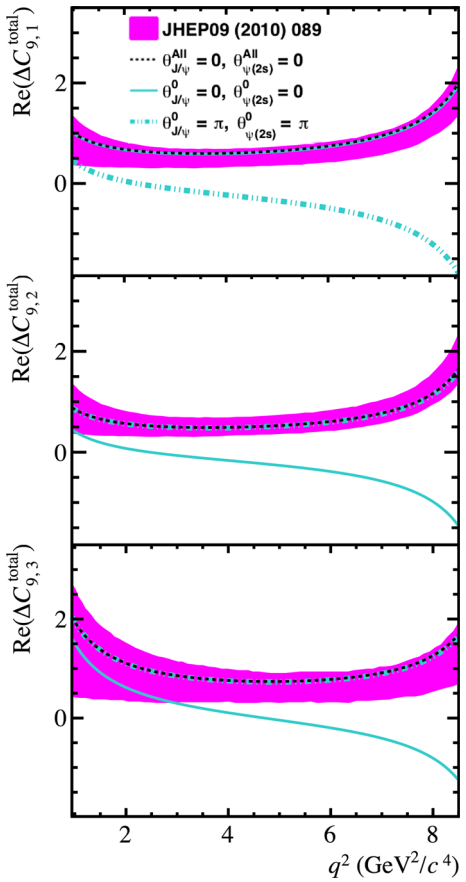

Fig. 1 The non-local contributions to the $B^0 \to K^{*0}\mu^+\mu^-$ invariant amplitudes as a function of q^2. The prediction using the model discussed in Sect. 2 is shown, where only the contributions from the J/ψ and $\psi(2S)$ resonances are considered. The free phases $\theta^0_{J/\psi}$ and $\theta^0_{\psi(2S)}$ are both set to 0 (cyan solid line) or π (cyan dashed-dotted line). The prediction where all phases of the J/ψ and $\psi(2S)$ appearing in Eqs. 7–9 are set to zero is also depicted (black solid line), alongside the prediction from Ref. [28] (magenta band)

to the helicity basis is also given in Ref. [28]. The predictions using the model described in Sect. 2, where only the contributions from the J/ψ and $\psi(2S)$ resonances are considered, are shown for comparison. The free phases $\theta^0_{J/\psi}$ and $\theta^0_{\psi(2S)}$ appearing in Eqs. 7–9 are both set to 0 or π. As a consistency check, the model presented in this paper is also shown, with the phases of all transversity amplitudes set to zero. The

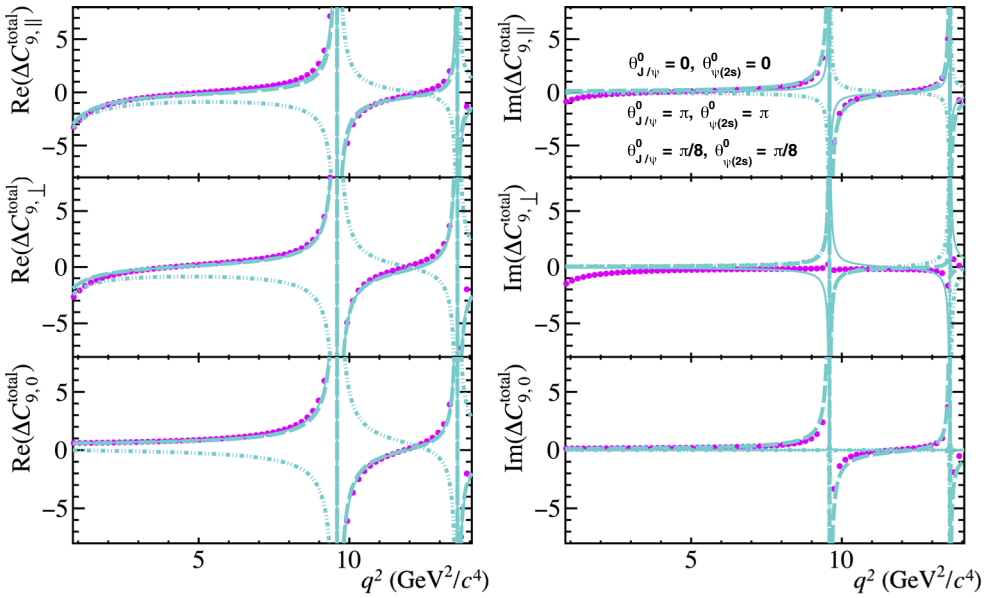

Fig. 2 The non-local contributions to the $\overline{B}^0 \to \overline{K}^{*0}\mu^+\mu^-$ transversity amplitudes as a function of q^2. The real (left) and imaginary (right) components are shown separately. The prediction from Ref. [21] is shown (magenta points). Predictions using the model discussed in Sect. 2, where only the contributions from the J/ψ and $\psi(2S)$ resonances are considered, are overlaid for different choices of the phases $\theta^0_{J/\psi}$ and $\theta^0_{\psi(2S)}$ (cyan lines). See text for further details

parameters ζ_λ and ω_λ also appearing in Eqs. 7–9 are chosen such that they are broadly consistent with the values of Ref. [15] and the predictions of Ref. [28], with $\zeta_\lambda \sim 0.08|C_7|$ and $\omega_\lambda = \pi$. Ignoring all phases of the transversity amplitudes of $\overline{B}^0 \to J/\psi\,\overline{K}^{*0}$ and $\overline{B}^0 \to \psi(2S)\overline{K}^{*0}$ decays, the model of $\Delta C_9^{\text{total}}_\lambda$ described in this analysis is consistent to that of Ref. [28]. However, accounting for the measured relative phases in the resonant decay amplitudes results in large differences between the two models. The level of disagreement depends on the value of the free phases $\theta^0_{J/\psi}$ and $\theta^0_{\psi(2S)}$. The effect of the non-local charm contributions in Ref. [28] are known to move the central value of predictions of angular observables such as P_5' further away from experimental measurements [16]. However, this effect is only true due to the fact that the analysis of Ref. [28] did not account for the phases of the resonant amplitudes. An assessment of the impact of the phases on the angular observables is discussed in Sect. 4.

Building on the ideas of Ref. [28], a recent analysis presented in Ref. [21] provides a prediction of the non-local charm contribution that is valid up to a $q^2 \leq m^2_{\psi(2S)}$. This prediction also makes use of experimental measurements of $\overline{B}^0 \to J/\psi\,\overline{K}^{*0}$ and $\overline{B}^0 \to \psi(2S)\overline{K}^{*0}$ decays. In contrast to Ref. [28], the calculations of the non-local contributions are performed at $q^2 < 0$ to next-to-leading order in α_s. The q^2 parametrisation is given by a z-expansion truncated after the second order as in Eq. (5). Figure 2 shows both the real and imaginary parts of the non-local contributions to $\overline{B}^0 \to \overline{K}^{*0}\mu^+\mu^-$ decays presented in Ref. [21]. As the correlations between the z-expansion parameters are not provided, only the central values of the predictions are shown. The phase convention used in Ref. [21] is such that the transversity amplitudes of the $\overline{B}^0 \to J/\psi\,\overline{K}^{*0}$ and $\overline{B}^0 \to \psi(2S)\overline{K}^{*0}$ decays are related to those presented in this study through $\eta_j^{\parallel} \to -\eta_j^{\parallel}$. The model described in Sect. 2, where only the contributions from the J/ψ and $\psi(2S)$ resonances are considered, is in qualitative agreement with that of Ref. [21] for the following parameter choice: $\theta^0_{J/\psi} = \pi/8$, $\theta^0_{\psi(2S)} = \pi/8$, $\zeta_\lambda \sim 15\%|C_7|$ and $\omega_\lambda = \pi$. The small level of disagreement observed in the imaginary part of the amplitudes at low q^2 is due to the choice of setting $\omega_\lambda = \pi$, with smaller values giving a better agreement.

To conclude, the simplistic model of the non-local contributions to $\overline{B}^0 \to \overline{K}^{*0}\mu^+\mu^-$ decays presented in this paper is in good agreement with existing models, provided appropriate choices of $\theta^0_{J/\psi}$, $\theta^0_{\psi(2S)}$, ω_λ and ζ_λ. For the latter, a larger value is required to match the predictions of Ref. [21], compared to Ref. [28]. The expressions of $\mathcal{G}_\lambda(q^2)$ have sufficient freedom to capture the q^2 dependence of formal theory predictions in the q^2 range $1 < q^2 < m^2_{\psi(2S)}$. In addition, in contrast to current predictions, the model of $\Delta C_9^{\text{total}}_\lambda(q^2)$ can naturally accommodate hadronic contributions from $J^{PC} = 1^{--}$ states composed of light quarks such as the ϕ and ρ^0, as well as resonances appearing in the region $q^2 > 4m_D^2$, where m_D denotes the mass of the D-meson. This is due to the use of Breit–Wigner functions to approximate the resonant contributions, that experiments can easily adopt.

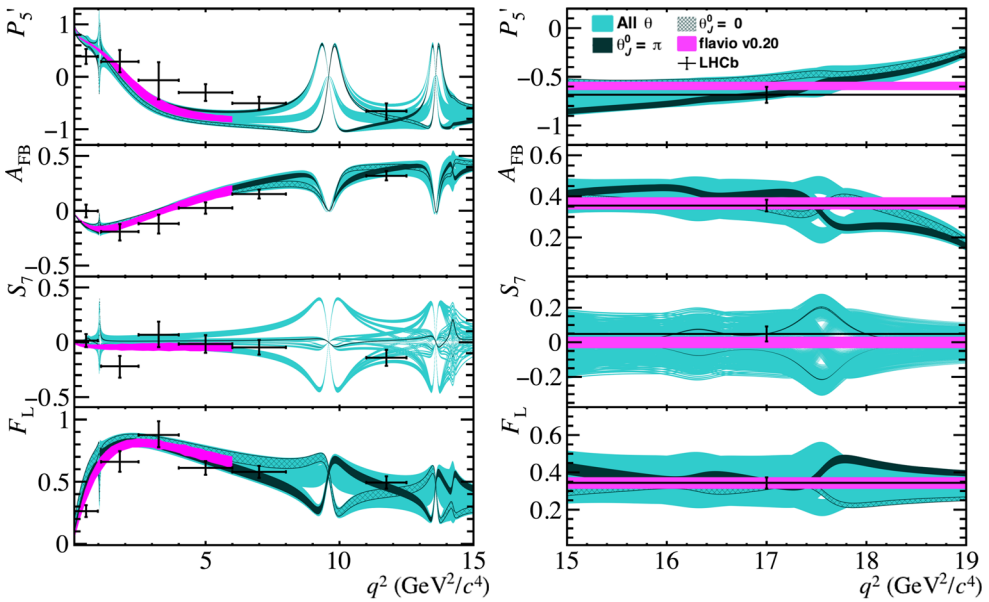

Fig. 3 Distributions of the angular observables P_5', $A_{\rm FB}$ S_7, and F_L as a function of q^2 for regions below (left) and above (right) the open charm threshold (cyan). Specific choices are highlighted for $\theta_j^0 = 0$ (hatched band) and $\theta_j^0 = \pi$ (dark band). The measured values of the observables from Ref. [49] are also shown (black points). The theoretical predictions (magenta band) using `flavio` [48] are shown for comparison

4 Effect on $\overline{B}^0 \to \overline{K}^{*0}\mu^+\mu^-$ angular observables

Using the model of $\Delta C_{9\,\lambda}^{\rm total}$ described in Sect. 2, the effect of the hadronic resonance contributions on the angular observables of $\overline{B}^0 \to \overline{K}^{*0}\mu^+\mu^-$ decays can be estimated. Figure 3 shows the distribution of the angular observables P_5', $A_{\rm FB}$, S_7 and F_L [45,46] in the SM. The observable S_7 exhibits a particularly large dependence on the strong phases, demonstrating that measurements of the angular distribution of $\overline{B}^0 \to \overline{K}^{*0}\mu^+\mu^-$ decays can be used to determine the phases of the hadronic resonances. Therefore, this observable can be used to separate short-distance from the non-local contributions, as only the non-local part has a strong-phase difference. The remaining CP-averaged observables can be found in Appendix B. Definitions of these observables can be found for instance in Ref. [47]. As the phase θ_j^0 of all the resonant final states appearing in Table 1 are unknown, all possible variations of phases θ_j^0 are considered. The uncertainties arising from the combined light-cone sum rules and lattice QCD calculations of $B \to K^*$ form factors are accounted for using the covariance matrix provided in Ref. [15]. The predictions of these observables using `flavio` [48] are also shown for comparison. The lack of knowledge of the phase θ_j^0 results in a large uncertainty for the prediction of P_5', diluting the sensitivity of this observable to the effects of physics beyond the SM. However, for the choice of θ_j^0 that results in a non-local charm contribution that is compatible with the latest prediction presented in Ref. [21] and is shown in Fig. 2), the tension of the prediction with the measured value of P_5' cannot be explained solely through hadronic effects.

4.1 Sensitivity to CP violation

The model of the hadronic resonance contributions to $\overline{B}^0 \to \overline{K}^{*0}\mu^+\mu^-$ decays described in this paper provides a prediction for the strong phase differences involved in these transitions. Direct CP violation will arise when there are interfering amplitudes that have different weak phases as well as different strong phases, as discussed within the context of $B^- \to K^-\mu^+\mu^-$ and $B^- \to \pi^-\mu^+\mu^-$ decays in Refs. [24,50]. Therefore, it is interesting to study the effect that potential weak phases beyond the SM have on angular observables such as the direct CP asymmetry A_{CP}, defined as

$$A_{CP} = \frac{\frac{d\Gamma(B \to K^*\mu^+\mu^-)}{dq^2} - \frac{d\overline{\Gamma}(B \to K^*\mu^+\mu^-)}{dq^2}}{\frac{d\Gamma(B \to K^*\mu^+\mu^-)}{dq^2} + \frac{d\overline{\Gamma}(B \to K^*\mu^+\mu^-)}{dq^2}}, \tag{12}$$

where Γ and $\overline{\Gamma}$ correspond to the partial widths of the decays $\overline{B}^0 \to \overline{K}^{*0}\mu^+\mu^-$ and $B^0 \to K^{*0}\mu^+\mu^-$ respectively, as well as the so-called CP-odd angular observables A_i, defined for instance in Ref. [36]. The method is similar to what is discusssed in Ref. [51] for semileptonic charm decays.

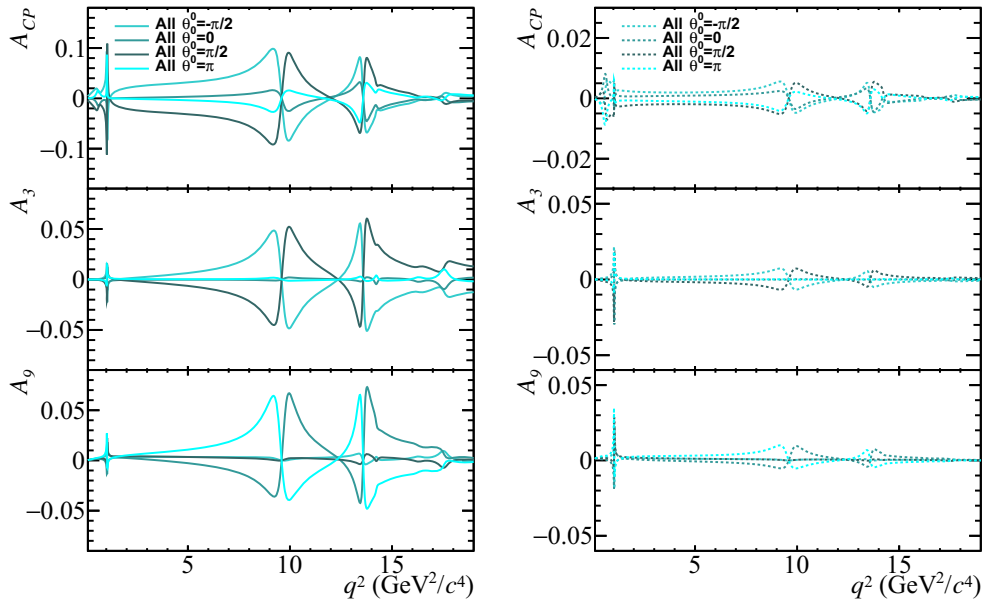

Fig. 4 Distribution of observables A_{CP}, A_3 and A_9 as a function of q^2, for θ_j^0 of all resonances set to $-\pi/2$, 0, $\pi/2$ and π. Two new physics models are considered, one with $C_9^{NP} = -1.0 - 1.0i$ (left), and one with $C_7^{NP} = -0.03i$, $C_9^{NP} = -1.0$ (right)

Figure 4 shows the observables A_{CP}, A_3 and A_9 for θ_j^0 of all resonances set to $-\pi/2$, 0, $\pi/2$ and π. To illustrate the effect that the model of the strong phase differences have in the presence of new weak phases, two new physics models are considered which are compatible with existing experimental constraints. One with $C_9^{\rm NP} = -1.0 - 1.0i$, and one with both $C_7^{\rm NP} = -0.03i$ and $C_9^{\rm NP} = -1.0$ [52,53]. The notation $C_{7,9}^{\rm NP}$ denotes the new physics contribution to the corresponding Wilson Coefficient. In both these models, all other Wilson Coefficients are set to their SM values. It is clear that the non-local contribution enhances CP-violating effects in these decays, with the level of this enhancement depending on the value of the unknown phase θ_j^0. As it can be seen, there is a huge effect in the vicinity of the resonances, thus giving sensitivity to an imaginary component of C_9 in a way which have not been considered before. The only other viable way to gain sensitivity would be through a time dependent analysis of the $B_s^0 \to J/\psi\,\phi$ or the $B^0 \to K^{*0}\mu^+\mu^-$ with the K^{*0} decaying to the CP eigenstate $K_S^0\pi^0$. In contrast, CP-violating effects arising through a weak phases appearing in the Wilson coefficient C_7, are best constrained from measurements of $B \to K^*\gamma$ decays [53].

4.2 Expected experimental precision

The experimental sensitivity to the phases between the short-range and hadronic resonance contributions to $\overline{B}^0 \to \overline{K}^{*0}\mu^+\mu^-$ is determined using $\mathcal{O}(10^6)$ simulated decays that include contributions from both short-distance and non-local components. The size of this sample corresponds to the approximate number of decays expected[2] to be collected by the LHCb experiment by the end of Run2 of the LHC [49]. The decays are generated with the parameters θ_j^0, ζ_λ and ω_λ set to zero. The S-wave contribution to $\overline{B}^0 \to \overline{K}^{*0}\mu^+\mu^-$ decays is accounted for using the angular terms and amplitude expressions as a function of the invariant mass of the $K\pi$ system given in Refs. [54,55]. In addition to the S-wave component for the short-range amplitude, S-wave components are introduced with an amplitude and phase (η_j^S, θ_j^S), for the J/ψ and the $\psi(2S)$ resonances, based on the measurements given in Refs. [29,30]. The overall effect of the S-wave contribution to the remaining resonances is considered to be negligible and is therefore ignored. In this study, all Wilson Coefficients are assumed to be real.

In order to ascertain the statistical precision on the non-local contribution, the detector resolution in q^2 needs to be accounted for by smearing the q^2 spectrum of the simulated events. For simplicity, a Gaussian resolution function is used with a width based on the RMS value of the dimuon mass resolution provided in Ref. [20], and converted into a resolution in q^2. As the resolution in the helicity angles are far better than the variations in the angular distributions, any resolution effect in angles can be ignored; the sharp shape of the ϕ, J/ψ and $\psi(2S)$ resonances mean that a similar argument is not valid for the q^2 distribution.

[2] The yield of both short-distance and non-local $\overline{B}^0 \to \overline{K}^{*0}\mu^+\mu^-$ decays is calculated by scaling the number of $\overline{B}^0 \to J/\psi\,\overline{K}^{*0}$ and short-distance $\overline{B}^0 \to \overline{K}^{*0}\mu^+\mu^-$ decays given in Ref. [49] by a factor of 4.

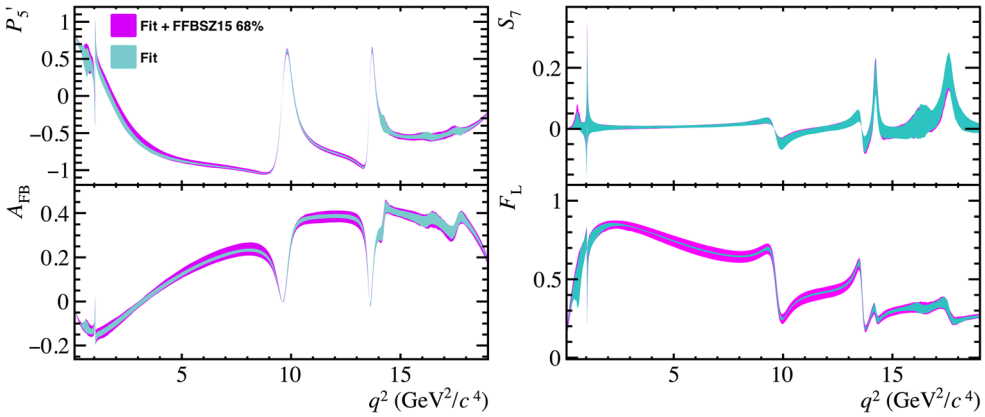

Fig. 5 Predictions of the observables P_5', $A_{\rm FB}$, S_7 and F_L in the SM using the expected post-fit precision of the non-local parameters $\Delta C_{9\,\lambda}^{\rm total}$ at the end of Run2 of the LHC. A sample of $\mathcal{O}(10^6)$ simulated $\overline{B}^0 \to \overline{K}^{*0}\mu^+\mu^-$ decays that include contributions from both short-distance and non-local components, is used to determine the parameters of $\Delta C_{9\,\lambda}^{\rm total}$. The decays are simulated in the SM, with the parameters θ_j^0, ζ_λ and ω_λ set to zero. The 68% confidence intervals are shown for the statistical uncertainty (cyan band) and the combination of the statistical uncertainty with the $B \to K^*$ form-factor uncertainties (magenta band) given in Ref. [15]

A four dimensional maximum likelihood fit is performed to the q^2, $\cos\theta_l$, $\cos\theta_K$ and ϕ distributions of the $\overline{B}^0 \to \overline{K}^{*0}\mu^+\mu^-$ decays in this sample. Both the non-local parameters, including η_j^S and θ_j^S, as well as the Wilson Coefficients C_9 and C_{10} are left to vary in the fit. The $B \to K^*$ form factor parameters however are fixed to their central values given in Ref. [15]. The resulting covariance matrix is used to ascertain the statistical precision on $\Delta C_{9\,\lambda}^{\rm total}$. Based on the assessment of the systematic uncertainties in Ref. [20], the dominant source of experimental uncertainty is expected to be statistical in nature. However, the presence of tetra-quark states appearing in $\overline{B}^0 \to K^-\pi^+ J/\psi$ and $\overline{B}^0 \to K^-\pi^+\psi(2S)$ decays [30,56] will impact the determination of the non-local parameters. Although the effect is expected to be small, an accurate assessment of the effect is beyond the scope of this study.

The statistical precision on the angular observables is estimated by generating values for the non-local parameters of $\Delta C_{9\,\lambda}^{\rm total}$, according to a multivariate Gaussian distribution centred at the values used to simulate the $\overline{B}^0 \to \overline{K}^{*0}\mu^+\mu^-$ decays, with a covariance matrix obtained from the resulting fit to the simulated data. These values are then propagated to the angular observables in order to obtain their 68% confidence interval as a function of q^2. Figure 5 shows the statistical precision to P_5', $A_{\rm FB}$, S_7 and F_L in the SM, where the non-local parameters are given by Table 1 with $\theta_j^0 = 0$. The equivalent plots for the remaining *CP*-averaged observables can be found in Appendix C.

By the end of Run2 of the LHC, the dominant theoretical uncertainty of the angular observables in the q^2 region $5 < q^2 < 14$ GeV$^2/c^4$, will be due to the knowledge of the $B \to K^*$ form-factors, rather than the non-local components. Future runs of the LHC will result in an even larger number of $\overline{B}^0 \to \overline{K}^{*0}\mu^+\mu^-$ decays. Therefore, it will, in a fit that combines the experimental data and the form factor uncertainties [57], be possible to use experimental data to further constrain Wilson Coefficients, as well as improve the precision of $B \to K^*$ form factors and non-local contributions from charm and light quark resonances.

5 Hadronic resonance effects in tests of lepton universality

Recent tests of lepton universality in $b \to s\ell^+\ell^-$ decays have revealed hints of non-universal new physics entering in the dimuon Wilson Coefficient C_9^μ [11,12,58,59]. The level of this potential new physics effect is compatible with the observed anomalies in the amplitude analyses and branching fraction measurements of $b \to s\mu^+\mu^-$ transitions. Lepton universality tests rely on measurements such as the ratios of branching fractions between decays with muons and electrons in the final state. The observables R_K and R_{K^*} are defined as

$$R_{K^{(*)}} = \frac{\int_{q^2_{min}}^{q^2_{max}} \frac{d\Gamma(B \to K^{(*)}\mu^+\mu^-)}{dq^2} dq^2}{\int_{q^2_{min}}^{q^2_{max}} \frac{d\Gamma(B \to K^{(*)}e^+e^-)}{dq^2} dq^2} \tag{13}$$

Hadronic effects in $b \to s\ell^+\ell^-$ decays are lepton universal and observables such as R_K and R_{K^*} can be predicted precisely in the SM, due to the cancellation of hadronic uncertainties. Therefore, any significant deviation between measurements and predictions of these quantities is a clear sign of physics beyond the SM. How-

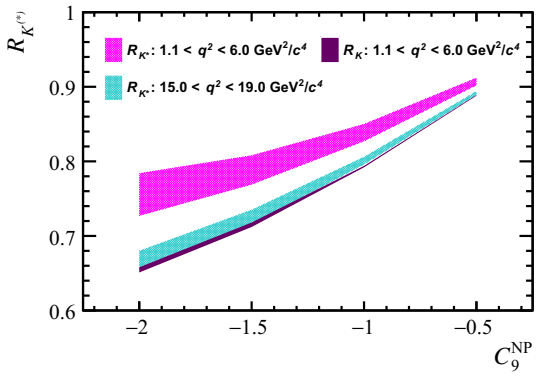

Fig. 6 Predictions of R_{K^*} at large recoil (hatched magenta) and low recoil (hatched cyan), and R_K at large recoil (solid burgundy) for different values of $C_{9\,\mu}^{\rm NP}$. The R_K values at low recoil are identical to those at large recoil and thus not shown. The interval for R_{K^*} is determined using the model described in Sect. 2, considering the full variation of the unknown phases θ_j^0. In contrast the 68% confidence interval of the R_K prediction is obtained using the measured non-local contributions in $B^- \to K^-\mu^+\mu^-$ decays [20]

ever, in the presence of new physics effects that enter through the Wilson Coefficient C_9^μ, the cancellation of hadronic uncertainties is no longer exact. Consequently, in order to determine the exact nature of any potential new physics model, an accurate determination of the non-local contributions in $\overline{B}^0 \to \overline{K}^{*0}\mu^+\mu^-$ decays is essential.

The model of $\Delta C_9^{\rm total}$ discussed in Sect. 2 is used to provide a prediction for R_{K^*} that accounts for the residual dependence on the unknown phases θ_j^0. Figure 6 summarises this prediction in models with values of $C_{9\,\mu}^{\rm NP}$ between -0.5 and -2.0, as suggested by global analyses of $b \to s\mu^+\mu^-$ transitions. The confidence interval for R_{K^*} is determined by considering the full variation of the unknown phases θ_j^0. The residual form factor uncertainty is found to be subdominant compared to the variation of the phase. A prediction for R_K is also provided, which uses the long distance contributions measured in Ref. [20] with the 68% confidence interval determined by treating the measured non-local parameters as uncorrelated. It can be seen that when the experimental data is used for measuring the phase of the non-local contribution, the residual uncertainty becomes very small. It is worth noting that for $C_{9\,\mu}^{\rm NP} = 0$, there is no dependence on the unknown phase θ_j^0. Tabulated values of these predictions can be found in Appendix D. In the presence of new physics entering the Wilson coefficient $C_{9\,\mu}$, a modest variation of R_{K^*} with the unknown phase θ_j^0 is observed. However, this variation is around 6 times smaller than the estimated uncertainty of R_{K^*} in the presence of lepton non-universal effects suggested by Ref. [11].

6 Conclusions

An empirical model to describe the hadronic resonance contributions in $\overline{B}^0 \to \overline{K}^{*0}\mu^+\mu^-$ transitions that relies on measurements of the branching fractions and polarisation amplitudes of $\overline{B}^0 \to V\overline{K}^{*0}$ decays, is presented. For a particular choice of the relative phases between the short-distance component and the hadronic amplitudes, this model was found to be in good agreement with more formal predictions such as those of Refs. [21,28]. The approach of this paper can naturally accommodate broad hadronic contributions from $J^{PC} = 1^{--}$ states such as the ρ^0, the ϕ and charm-resonances above the open charm threshold, which can be inserted into experimental analyses of $\overline{B}^0 \to \overline{K}^{*0}\mu^+\mu^-$ decays.

The lack of knowledge of the longitudinal phase differences between $\overline{B}^0 \to \overline{K}^{*0}\mu^+\mu^-$ and $B^0 \to V\overline{K}^{*0}$ decays results in a larger uncertainty on the predictions of the angular observables of $\overline{B}^0 \to \overline{K}^{*0}\mu^+\mu^-$ decays compared to current approaches. A measurement of these phases is critical as it will reduce the uncertainty in the determination of the Wilson Coefficients.

In addition, the resonant contributions to the decay provide large strong-phase differences that enhance sensitivity to CP violating effects. In this way, there is no need to rely on a time dependent analysis to a *CP* eigenstate. For the method to be exploited, it is required to have a model of the strong phase differences between short- and non-local contributions to $\overline{B}^0 \to \overline{K}^{*0}\mu^+\mu^-$ transitions as proposed here.

In the SM, observables such as R_K and R_{K^*} are independent of hadronic uncertainties. However, in the presence of non-universal effects in $b \to s\,\ell^+\ell^-$ transitions, these observables receive uncertainties from both the form-factor calculations and the interference between short- and non-local amplitudes. Using the models described in Ref. [20] and in this paper, predictions for R_K and R_{K^*} are provided for various choices of the Wilson coefficient C_9^μ. In order to maximise the potential of observables such as R_{K^*} as a way of characterising the exact physics model behind potential lepton-universality violating effects, a measurement of the non-local contributions in $\overline{B}^0 \to \overline{K}^{*0}\mu^+\mu^-$ decays is crucial. The data sample that will be collected by the LHCb experiment by the end of Run2 of the LHC will allow for a simultaneous amplitude analysis of both short-distance and non-local contributions to $\overline{B}^0 \to \overline{K}^{*0}\mu^+\mu^-$ decays across the full q^2 spectrum of the decay. The model described in this paper, allows for a precise determination of both of these components.

Acknowledgements We would like to thank C. Bobeth, D. van Dyk, and J. Virto for their help in obtaining their predictions of the charm correlator and for explaining in detail their model. We would also like to thank J. Matias, A. Khodjamirian and R. Zwicky for helpful discussions. Many thanks to S. Harnew, C. Langenbruch, S. Maddrell-Mander,

J. Rademacker, M.-H. Schune and N. Skidmore for their corrections to the text. GP acknowledges support from the UK Science and Technology Facilities Council (STFC) from the Grant ST/N503952/1, TB acknowledges support from the Royal Society (United Kingdom) and PO acknowledges support from the Swiss National Science Foundation under grant number BSSGI0_155990.

Funded by SCOAP[3].

Appendix

A Normalisation of the η_j^λ parameters

The magnitude of each resonant amplitude η_j^λ appearing in Eqs. (7–9) is given by

$$
\begin{aligned}
|\eta_j^0|^2 &= \frac{f_j^0 \mathcal{B}(\overline{B}^0 \to V\overline{K}^{*0}) \times \mathcal{B}(V \to \mu^+\mu^-)}{\tau_B \int \left| 8N \frac{m_B m_{K^*}}{\sqrt{q^2}} A_j^{\rm res}(q^2) A_{12}(q^2) \right|^2 dq^2}, \\
|\eta_j^\parallel|^2 &= \frac{f_j^\parallel \mathcal{B}(\overline{B}^0 \to V\overline{K}^{*0}) \times \mathcal{B}(V \to \mu^+\mu^-)}{\tau_B \int \left| N\sqrt{2}(m_B^2 - m_{K^*}^2) A_j^{\rm res}(q^2) \frac{A_1(q^2)}{m_B - m_{K^*}} \right|^2 dq^2}, \\
|\eta_j^\perp|^2 &= \frac{f_j^\perp \mathcal{B}(\overline{B}^0 \to V\overline{K}^{*0}) \times \mathcal{B}(V \to \mu^+\mu^-)}{\tau_B \int \left| N\sqrt{2\lambda} A_j^{\rm res}(q^2) \frac{V(q^2)}{m_B + m_{K^*}} \right|^2 dq^2},
\end{aligned}
\tag{14}
$$

where the f_j^λ factors denote the measured polarisation fraction of $\overline{B}^0 \to V\overline{K}^{*0}$ decays and τ_B denotes the B-meson lifetime.

B *CP*-averaged observables

See Fig. 7

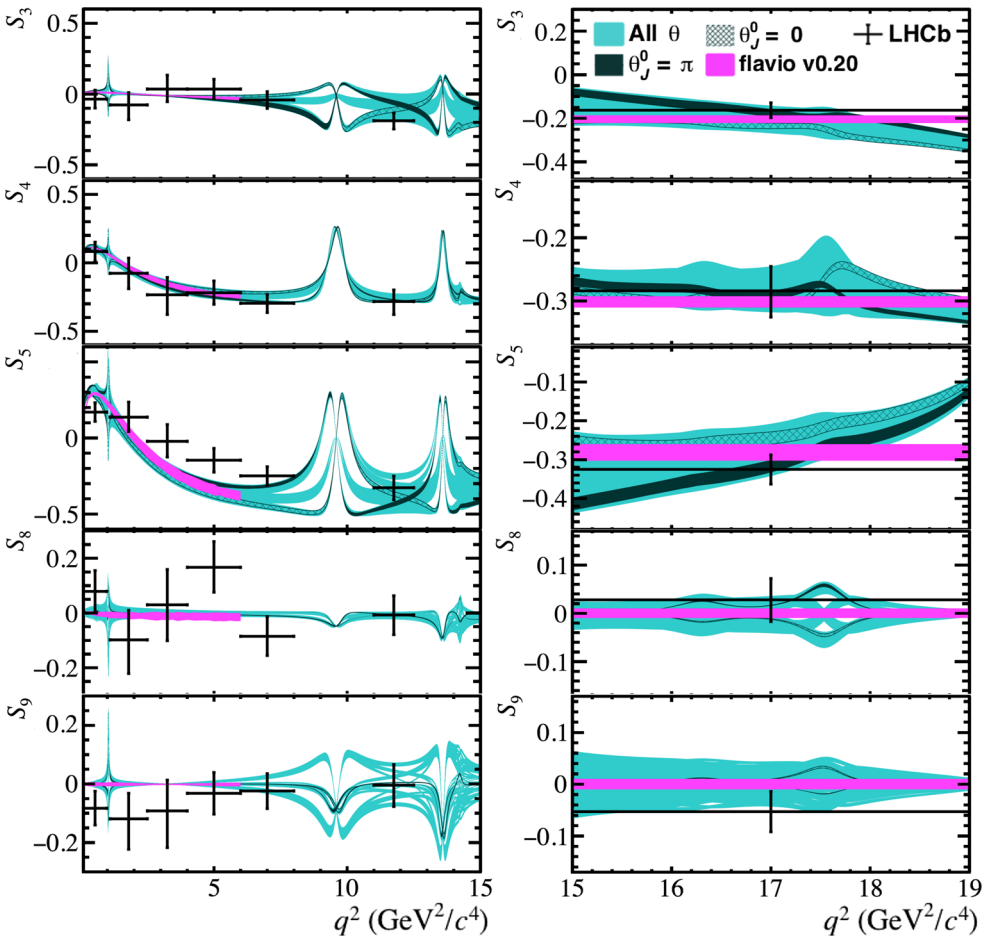

Fig. 7 Distributions of the *CP*-averaged observables in the SM as a function of q^2 below (left) and above (right) the open charm threshold (cyan). Specific choices are highlighted for $\theta_j^0 = 0$ (hatched band) and $\theta_j^0 = \pi$ (dark band). The measured values of the observables from Ref. [49] are also shown (black points). The theoretical predictions (magenta band) using `flavio` [48] are shown for comparison

C Experimental sensitivity for *CP*-averaged observables

See Fig. 8

D R_{K^*} and R_K predictions

See Table 2

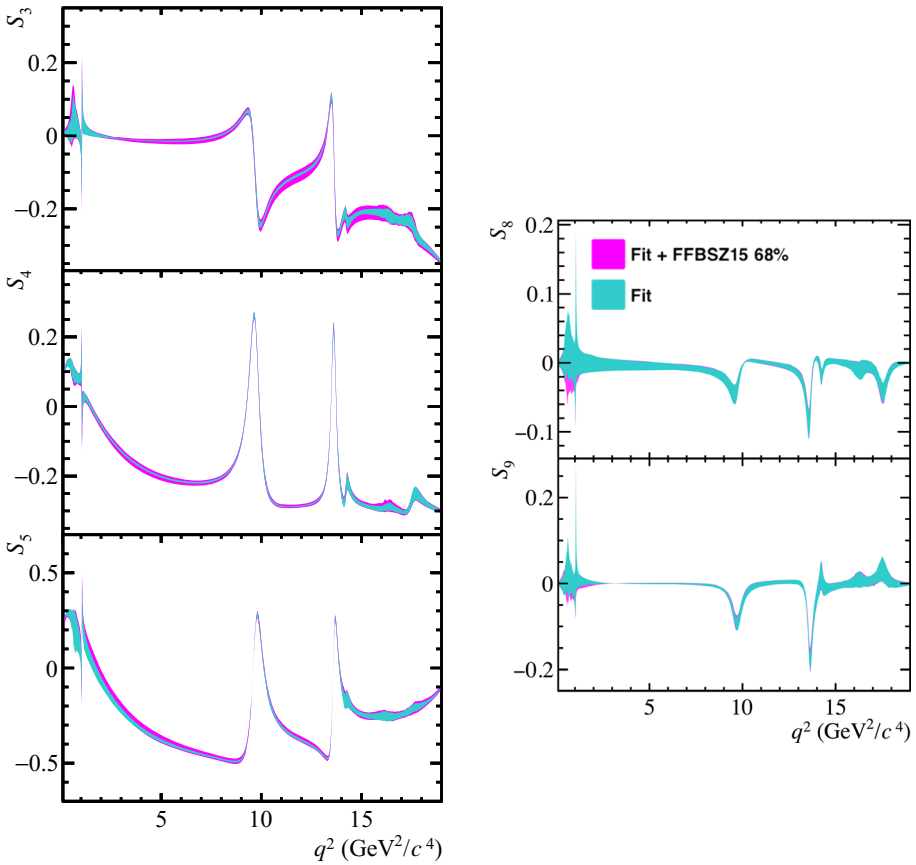

Fig. 8 Predictions of the remaining *CP*-averaged observables in the SM using the expected post-fit precision of the long-distance parameters $\Delta C_{9\,\lambda}^{\text{total}}$ at the end of Run2 of the LHC. A sample of $\mathcal{O}(10^6)$ simulated $\overline{B}^0 \to \overline{K}^{*0}\mu^+\mu^-$ decays that include contributions from both short- and long-distance components, is used to determine the parameters of $\Delta C_{9\,\lambda}^{\text{total}}$. The decays are simulated in the SM, with the parameters θ_j^0, ζ_λ and ω_λ set to zero. The 68% confidence intervals are shown for the statistical uncertainty (cyan band) and the combination of the statistical uncertainty with the $B \to K^*$ form-factor uncertainties (magenta band) given in Ref. [15]

Table 2 Predictions of R_{K^*} and R_K at large and low recoil for different values of $C_{9\,\mu}^{\text{NP}}$. The interval for R_{K^*} is determined using the model described in Sect. 2, considering the full variation of the unknown phases θ_j^0. The uncertainty due to the residual form factor dependence is found to be subdominant. In contrast, the 68% confidence interval of the R_K prediction is obtained using the measured long distance contributions in $B^- \to K^-\mu^+\mu^-$ decays [20]

Observable	$C_{9\,\mu}^{\text{NP}} = -0.5$	$C_{9\,\mu}^{\text{NP}} = -1.0$	$C_{9\,\mu}^{\text{NP}} = -1.5$	$C_{9\,\mu}^{\text{NP}} = -2.0$
	$1.1 < q^2 < 6.0$ GeV$^2/c^4$			
R_{K^*}	[0.902, 0.912]	[0.827, 0.850]	[0.769, 0.808]	[0.727, 0.784]
R_K	[0.888, 0.889]	[0.792, 0.794]	[0.712, 0.718]	[0.651, 0.658]
	$15 < q^2 < 19$ GeV$^2/c^4$			
R_{K^*}	[0.889, 0.894]	[0.796, 0.806]	[0.719, 0.735]	[0.658, 0.680]
R_K	[0.888, 0.889]	[0.792, 0.794]	[0.712, 0.718]	[0.651, 0.658]

References

1. CMS collaboration, Measurement of the P_1 and P_5' angular parameters of the decay $B^0 \to K^{*0}\mu^+\mu^-$ in proton-proton collisions at $\sqrt{s} = 8$TeV, CMS-PAS-BPH-15-008, (2017)
2. ATLAS collaboration, Angular analysis of $B_d^0 \to K^*\mu^+\mu^-$ decays in pp collisions at $\sqrt{s} = 8$ TeV with the ATLAS detector, ATLAS-CONF-2017-023, (2017)
3. Belle collaboration, S. Wehle et al., Lepton-Flavor-Dependent Angular Analysis of $B \to K^*\ell^+\ell^-$. Phys. Rev. Lett. **118** (2017) 111801. arXiv:1612.05014
4. LHCb collaboration, R. Aaij et al., Measurement of the S-wave fraction in $B^0 \to K^+\pi^-\mu^+\mu^-$ decays and the $B^0 \to k^*(892)^0\mu^+\mu^-$ differential branching fraction. JHEP **11** (2016) 047. arXiv:1606.04731 (**Erratum ibid. textbf04 (2017) 142**)
5. LHCb collaboration, R. Aaij et al., Measurement of the branching fraction ratio and CP asymmetry difference of the decays $B^+ \to J/\psi\pi^+$ and $B^+ \to J/\psi K^+$. JHEP **03** (2017) 036. arXiv:1612.06116
6. LHCb collaboration, R. Aaij et al., Angular analysis and differential branching fraction of the decay $B_s^0 \to \phi\mu^+\mu^-$. JHEP **09** (2015) 179. arXiv:1506.08777
7. CMS collaboration, V. Khachatryan et al., Angular analysis of the decay $B^0 \to K^{*0}\mu^+\mu^-$ from pp collisions at $\sqrt{s} = 8$ TeV. Phys. Lett. B **753** (2016) 424. arXiv:1507.08126
8. BaBar collaboration, J.P. Lees et al., Measurement of angular asymmetries in the decays $B \to K^*\ell^+\ell^-$. Phys. Rev. D **93** (2016) 052015. arXiv:1508.07960
9. LHCb collaboration, R. Aaij et al., Angular analysis of charged and neutral $B \to K\mu^+\mu^-$ decays. JHEP **05** (2014) 082. arXiv:1403.8045
10. LHCb collaboration, R. Aaij et al., Differential branching fractions and isospin asymmetries of $B \to K^*\mu^+\mu^-$ decays. JHEP **06** (2014) 133. arXiv:1403.8044
11. B. Capdevila et al., Patterns of new physics in $b \to s\ell^+\ell^-$ transitions in the light of recent data. arXiv:1704.05340
12. W. Altmannshofer, C. Niehoff, P. Stangl, D.M. Straub, Status of the $B \to K^*\mu^+\mu^-$ anomaly after Moriond 2017. Eur. Phys. J. C **77**, 377 (2017). arXiv:1703.09189
13. T. Hurth, F. Mahmoudi, S. Neshatpour, On the anomalies in the latest LHCb data. Nucl. Phys. B **909**, 737 (2016). arXiv:1603.00865
14. W. Altmannshofer, D.M. Straub, New physics in $b \to s$ transitions after LHC run. Eur. Phys. J. **C75**(8), 382 (2015). arXiv:1411.3161
15. A. Bharucha, D.M. Straub, R. Zwicky, $B \to V\ell^+\ell^-$ in the Standard Model from light-cone sum rules. JHEP **08**, 098 (2016). arXiv:1503.05534
16. S. Descotes-Genon, L. Hofer, J. Matias, J. Virto, Global analysis of $b \to s\ell\ell$ anomalies. JHEP **06**, 092 (2016). arXiv:1510.04239
17. F. Beaujean, C. Bobeth, D. van Dyk, Comprehensive Bayesian analysis of rare (semi)leptonic and radiative B decays. Eur. Phys. J. C **74**, 2897 (2014). arXiv:1310.2478
18. J. Lyon, R. Zwicky, Resonances gone topsy turvy - the charm of QCD or new physics in $b \to s\ell^+\ell^-$?. arXiv:1406.0566
19. S. Braß, G. Hiller, I. Nisandzic, Zooming in on $B \to K^*\ell\ell$ decays at low recoil. Eur. Phys. J. C **77**, 16 (2017). arXiv:1606.00775
20. LHCb collaboration, R. Aaij et al., Measurement of the phase difference between the short- and long-distance amplitudes in the $B^+ \to K^+\mu^+\mu^-$ decay. Eur. Phys. J. C **77** (2017) 161. arXiv:1612.06764
21. C. Bobeth, M. Chrzaszcz, D. van Dyk, J. Virto, Long-distance effects in $B \to K^*\ell\ell$ from Analyticity. arXiv:1707.07305
22. B. Capdevila, S. Descotes-Genon, L. Hofer, J. Matias, Hadronic uncertainties in $B \to K^*\mu^+\mu^-$: a state-of-the-art analysis. JHEP **04**, 016 (2017). arXiv:1701.08672
23. S. Jäger, K. Leslie, M. Kirk, A. Lenz, Charming new physics in rare B-decays and mixing? arXiv:1701.09183
24. A. Khodjamirian, A. V. Rusov, $B_s \to K\ell\ell$ and $B_{(s)} \to \pi(K)\ell^+\ell^-$ decays at large recoil and CKM matrix elements. arXiv:1703.04765
25. M. Ciuchini et al., $B \to K^*\ell^+\ell^-$ decays at large recoil in the Standard Model: a theoretical reappraisal. JHEP **06**, 116 (2016). arXiv:1512.07157
26. S. Jäger, J. Martin Camalich, On $B \to Vll$ at small dilepton invariant mass, power corrections, and new physics. JHEP **05** (2013) 043. arXiv:1212.2263
27. A. Khodjamirian, T. Mannel, Y.M. Wang, $B \to K\ell^+\ell^-$ decay at large hadronic recoil. JHEP **02**, 010 (2013). arXiv:1211.0234
28. A. Khodjamirian, T. Mannel, A.A. Pivovarov, Y.-M. Wang, Charm-loop effect in $B \to K^{(*)}\ell^+\ell^-$ and $B \to K^*\gamma$. JHEP **09**, 089 (2010). arXiv:1006.4945
29. LHCb collaboration, R. Aaij et al., Updated measurements of exclusive J/ψ and $\psi(2S)$ production cross-sections in pp collisions at $\sqrt{s} = 7$Tev. J. Phys. G **41** (2014) 055002. arXiv:1401.3288
30. Belle collaboration, K. Chilikin et al., Experimental constraints on the spin and parity of the $Z(4430)^+$. Phys. Rev. D **88** (2013) 074026. arXiv:1306.4894
31. BaBar Collaboration, B. Aubert et al., Measurement of decay amplitudes of $B \to J/\psi K^*$, $\psi(2S)K^*$, and $\chi_{c1}K^*$ with an angular analysis. Phys. Rev. D **76**, 031102 (2007). arXiv:0704.0522
32. Belle collaboration, K. Chilikin et al., Observation of a new charged charmonium like state in $\bar{B}^0 \to J/\psi K^-\pi^+$ decays, Phys. Rev. D **90** (2014) 112009, arXiv:1408.6457
33. LHCb collaboration, R. Aaij et al., Test of lepton universality with $B^0 \to K^{*0}\ell^+\ell^-$ decays. JHEP **08** (2017) 055. arXiv:1705.05802
34. LHCb collaboration, R. Aaij et al., Test of lepton universality using $B^+ \to K^+\ell^+\ell^-$ decays. Phys. Rev. Lett. **113** (2014) 151601. arXiv:1406.6482
35. U. Egede et al., New observables in the decay mode $\bar{B}^0 \to \bar{K}^{*0}\ell^+\ell^-$. JHEP **11**, 032 (2008). arXiv:0807.2589
36. W. Altmannshofer et al., Symmetries and asymmetries of $B \to K^*\mu^+\mu^-$ Decays in the Standard Model and beyond. JHEP **0901**, 019 (2009). arXiv:0811.1214
37. R.R. Horgan, Z. Liu, S. Meinel, M. Wingate, Lattice QCD calculation of form factors describing the rare decays $B \to K^*\ell^+\ell^-$ and $B_s \to \phi\ell^+\ell^-$. Phys. Rev. D **89**, 094501 (2014). arXiv:1310.3722
38. C. Patrignani, P.D. Group, Review of particle physics. Chin. Phys. C **40**, 100001 (2016)
39. LHCb Collaboration, R. Aaij et al., Measurement of the polarization amplitudes in $B^0 \to J/\psi\ K^*(892)^0$ decays. Phys. Rev. D. **88** (2013) 052002. arXiv:1307.2782
40. LHCb collaboration, R. Aaij *et al.*, Measurement of polarization amplitudes and CP asymmetries in $B^0 \to \phi K^*(892)^0$, JHEP **05** (2014) 069 CERN-PH-EP-2014-038, LHCb-PAPER-2014-005, arXiv:1403.2888
41. Belle collaboration, M. Prim et al., Angular analysis of $B^0 \to \phi K^*$ decays and search for CP violation at Belle. Phys. Rev. D **88** (2013) 072004. arXiv:1308.1830
42. BaBar collaboration, B. Aubert et al., Time-dependent and time-integrated angular analysis of $B \to \phi K_s\pi^0$ and $B \to \phi K^+\pi^-$. Phys. Rev. D **78** (2008) 092008. arXiv:0808.3586
43. BaBar collaboration, J.P. Lees et al., B^0 meson decays to $\rho^0 K^{*0}$, $f_0 K^{*0}$, and $\rho^- K^{*+}$, including higher K^* resonances. Phys. Rev. D **85** (2012) 072005. arXiv:1112.3896
44. Belle collaboration, S.-H. Kyeong et al., Measurements of charmless hadronic $b \to s$ penguin decays in the $\pi^+\pi^-\ K^+pi^-$ final state and observation of $B^0 \to \rho^0 K^+pi^-$. Phys. Rev. D **80** (2009) 051103. arXiv:0905.0763
45. S. Descotes-Genon, J. Matias, M. Ramon, J. Virto, Implications from clean observables for the binned analysis of $B \to K^*\mu^+\mu^-$ at large recoil. JHEP **01**, 048 (2013). arXiv:1207.2753

46. F. Kruger, L.M. Sehgal, N. Sinha, R. Sinha, Angular distribution and CP asymmetries in the decays $\bar{B} \to K^-\pi^+e^-e^+$ and $\bar{B} \to \pi^-\pi^+e^-e^+$, Phys. Rev. D **61**, 114028 (2000). arXiv:hep-ph/9907386 (**Erratum ibid. D63(2001), 019901**)
47. S. Descotes-Genon, T. Hurth, J. Matias, J. Virto, Optimizing the basis of $B \to K^*\ell^+\ell^-$ observables in the full kinematic range. JHEP **1305**, 137 (2013). arXiv:1303.5794
48. D. Straub et al., flav-io/flavio v0.20, (2017). https://doi.org/10.5281/zenodo.375591
49. LHCb collaboration, R. Aaij et al., Angular analysis of the $B^0 \to K^*\mu+\mu^-$ decay using $3\,fb^{-1}$ of integrated luminosity. JHEP **02** (2016) 104. arXiv:1512.04442
50. C. Hambrock, A. Khodjamirian, A. Rusov, Hadronic effects and observables in $B \to \pi\ell^+\ell^-$ decay at large recoil. Phys. Rev. D **92**, 074020 (2015). arXiv:1506.07760
51. S. Fajfer, N. Košnik, Resonance catalyzed CP asymmetries in $D \to P\ell^+\ell^-$. Phys. Rev. D **87**, 054026 (2013). arXiv:1208.0759
52. A.K. Alok et al., New physics in $b \to s\mu^+\mu^-$: Distinguishing models through CP-violating effects. Phys. Rev. D **96**, 015034 (2017). arXiv:1703.09247
53. A. Paul, D.M. Straub, Constraints on new physics from radiative B decays. JHEP **04**, 027 (2017). arXiv:1608.02556
54. C.-D. Lü, W. Wang, Analysis of $B \to K_J^*(\to K\pi)\mu^+\mu^-$ in the higher kaon resonance region. Phys. Rev. D **85**, 034014 (2012). arXiv:1111.1513
55. U.-G. Meisner, W. Wang, Generalized heavy-to-light form factors in light-cone sum rules. Phys. Lett. B **730**, 336 (2014). arXiv:1312.3087
56. LHCb, R. Aaij et al., Observation of the resonant character of the $Z(4430)^-$ state. Phys. Rev. Lett. **112** (2014) 222002. arXiv:1404.1903
57. T. Hurth, C. Langenbruch, F. Mahmoudi, Direct determination of Wilson coefficients using $B^0 \to K^{*0}\mu^+\mu^-$ decays. arXiv:1708.04474
58. L.-S. Geng et al., Towards the discovery of new physics with lepton-universality ratios of $b \to s\ell\ell$ decays. arXiv:1704.05446
59. M. Ciuchini et al., On flavourful easter eggs for new physics hunger and lepton flavour universality violation. arXiv:1704.05447